

# Organic & Biomolecular Chemistry

Accepted Manuscript

This article can be cited before page numbers have been issued, to do this please use: D. Mori, T. Yoneda, M. Suzuki, T. Hoshino and S. Neya, *Org. Biomol. Chem.*, 2020, DOI: 10.1039/D0OB01213K.



This is an Accepted Manuscript, which has been through the Royal Society of Chemistry peer review process and has been accepted for publication.

Accepted Manuscripts are published online shortly after acceptance, before technical editing, formatting and proof reading. Using this free service, authors can make their results available to the community, in citable form, before we publish the edited article. We will replace this Accepted Manuscript with the edited and formatted Advance Article as soon as it is available.

You can find more information about Accepted Manuscripts in the [Information for Authors](#).

Please note that technical editing may introduce minor changes to the text and/or graphics, which may alter content. The journal's standard [Terms & Conditions](#) and the [Ethical guidelines](#) still apply. In no event shall the Royal Society of Chemistry be held responsible for any errors or omissions in this Accepted Manuscript or any consequences arising from the use of any information it contains.

## COMMUNICATION

Deprotection of benzyl unit induces 22 $\pi$  aromatic macrocycle of 3-oxypyripenaphyrin(0.1.1.1.0) with strong NIR absorption.Daiki Mori<sup>a</sup>, Tomoki Yoneda<sup>a,b\*</sup>, Masaaki Suzuki<sup>c</sup>, Tyuji Hoshino<sup>a</sup>, and Saburo Neya<sup>a\*</sup>Received 00th January 20xx,  
Accepted 00th January 20xx

DOI: 10.1039/x0xx00000x

We report aromaticity switching from a 6 $\pi$  pyridine ring to 22 $\pi$  macrocyclic ring of 3-oxypyripenaphyrin(0.1.1.1.0). This system has potential applications in photodynamic therapy owing to macrocyclic aromaticity being selectively induced by protecting group removal and strong absorption bands produced in the NIR region especially in methanol.

Porphyrins and their analogs are employed for photodynamic therapy (PDT), which is a treatment used to eliminate cancer or abnormal tissue lesions.<sup>1</sup> Conventional porphyrin photosensitisers have their longest absorption maxima in the visible-light range. However, regarding penetration depth, photosensitiser with absorbance of NIR region (700–1100 nm) is desired.<sup>2</sup> Expanded porphyrins with large  $\pi$ -conjugation circuits<sup>3</sup> which absorb light reaching NIR region are expected for application of photodynamic therapy.<sup>4</sup> However, a known undesirable side effect of existing photosensitisers is phototoxicity toward healthy tissue. This problem can be more serious when expanded porphyrins with strong absorption in the visible and NIR regions are adopted as photosensitisers. If the strong NIR absorption of a molecule is induced by deprotection, this system can be a candidate of photosensitizer. This system prevents photosensitivity toward ambient light until metabolization occurs in tumors or tissue lesions. The removal of protecting group is theoretically applicable to new reagents for NIR photodynamic therapy by employing appropriate protecting groups metabolised in tumour. If the aromaticity of expanded porphyrins could also be triggered by metabolization, the molecule would show strong NIR absorption and be a theoretically crucial candidates for photodynamic therapy would be obtained (Fig. 1).

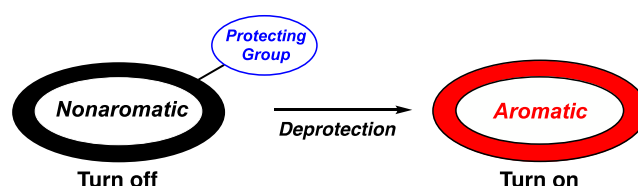
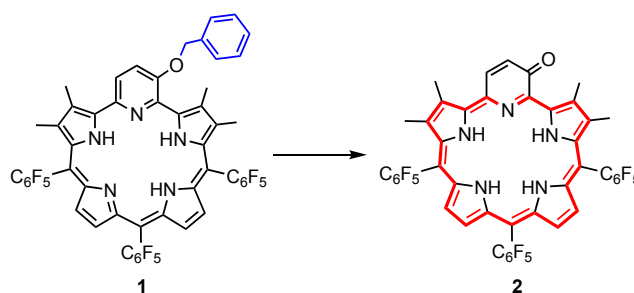


Fig. 1. Representation of "Deprotection Induced Aromaticity" strategy.



Scheme 1. Aromaticity induced by deprotection of 1.

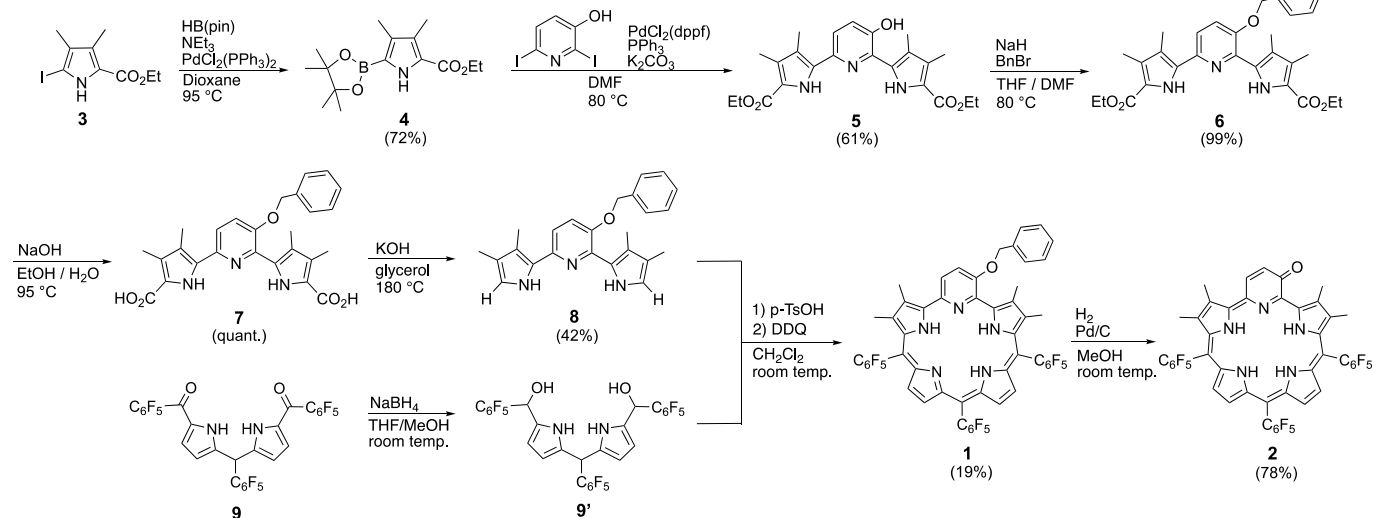
As the example of such expanded porphyrin systems, we herein report an expanded porphyrin with macrocyclic aromaticity which is triggered by simple benzyl group deprotection. We designed deprotection of 3-benzyloxyripenaphyrin(0.1.1.1.0) **1** to produce 3-oxypyripenaphyrin(0.1.1.1.0) **2** as an expanded porphyrin system with 3-oxypyridine ring (Scheme 1). Reported pentaphyrin(1.1.1.0.0)s with five pyrrole rings are known to have aromatic character derived from their 22 $\pi$  conjugation circuits.<sup>5</sup> To improve the stability of such electron-rich pentaphyrins, we suggested installing a pyridine ring instead of pyrrole. Compared with pyrrole, in which 6 $\pi$ -electrons are delocalised on five atoms, the pyridine ring is more electron-deficient because of delocalisation of same number of electrons on six atoms. As pyridine-containing porphyrins, macrocycles bearing pyridine or 3-oxypyridine rings have been reported. Among them, pyridine rings without substituents at  $\beta$ - or  $\gamma$ -positions favour aromaticity of 6 $\pi$  pyridine rings, with their macrocyclic aromaticity connected in

<sup>a</sup> Department of Pharmaceutical Sciences, Chiba University  
Inohana, Chuo-ku, Chiba, 260-8675, Japan.

<sup>b</sup> Division of Applied Chemistry, Faculty of Engineering, Hokkaido University, Kita 13  
Nishi 8 Kita-ku, Sapporo, Hokkaido, 060-8628, Japan,  
E-mail: t\_yoneda@eng.hokudai.ac.jp.

<sup>c</sup> Graduate School of Natural Science and Technology, Shimane University  
1060, Nishikawatsu-cho, Matsue, Shimane, 690-8504, Japan

Electronic Supplementary Information (ESI) available: [details of any supplementary information available should be included here]. See DOI: 10.1039/x0xx00000x

Scheme 2. Synthetic procedure of 3-oxypyripyentaphyrins **1** and **2**.

a cross-conjugated manner.<sup>6</sup> In contrast, in molecules with 3-oxopyridine (pyridone) rings, macrocyclic 18 $\pi$  aromaticity takes priority over aromaticity of 6 $\pi$  pyridine ring.<sup>7</sup> The similar system of 3-hydroxybenzporphyrins and the induction of aromaticity by deprotection of methyl group was also reported.<sup>8</sup> From these previous researches, the usage of 3-oxopyridine ring can be effectively induce aromaticity in expanded porphyrin macrocycles. Previously, Setsune *et al.* reported expanded porphyrins containing pyridine moieties in their structure, although these molecules did not show macrocyclic aromaticity.<sup>9</sup> Sessler *et al.* also reported the synthesis of cyclo[m]pyridine[n]pyrroles, which showed aromaticity only under acidic conditions.<sup>10</sup> In addition, pyrrole and pyridine moieties of **1** have been designed to prevent *meso*-carbon oxygenation.<sup>11</sup>

The synthetic procedure for **1** is shown in Scheme 2. To synthesise the desired 3-oxypyripyentaphyrin(0.1.1.1.0), we designed the synthesis of directly connected pyrrole-pyridine-pyrrole (dipyrropyridine) moiety known in the synthesis of expanded pyriporphyrins.<sup>9,12</sup> Using Miyaura-Ishiyama borylation, 2-ethoxycarbonyl-5-iodo-3,4-dimethylpyrrole **3** was transformed into a borylated analog **4** in 72% yield. Compound **4** (2 equiv.) was coupled with 2,6-diiodopyridin-3-ol to afford a new directly bonded pyrrole-pyridine-pyrrole trimer **5** in 61% yield. The hydroxyl group of **5** was protected with benzyl bromide to give benzyl ether **6** quantitatively. The terminal ethoxycarbonyl groups of **6** were completely hydrolysed by saponification affording **7** quantitatively. Without the protection of hydroxyl group, the saponification of **5** produced a complex mixture and corresponding carboxylic acid was not obtained at all. Through decarboxylation using NaOH and glycerol at 180 °C, dipyrropyridine **8** was obtained in 42% yield. Trimer **8** was condensed with pentafluorophenyl-substituted dipyrromethane dicarbinol **9'**, which was prepared from the reduction of acyl precursor **9**. Similarly to our reported procedure of the synthesis of pyripyentaphyrin,<sup>11</sup> acid-catalysed

condensation using *p*-toluenesulfonic acid (1.3 equiv.) followed by oxidation with 2,3-dichloro-5,6-dicyano-1,4-benzoquinone (DDQ; 3.0 equiv) afforded benzyl-protected pyripyentaphyrin(0.1.1.1.0) **1** in 19% yield. The benzyl group of **1** was intact under the oxidative conditions.

High-resolution electrospray ionization mass spectroscopy (HR-ESI-TOF-MS) provided the parent ion peak of **1** at  $m/z$  = 1036.2133 (calcd for 1036.2128). The <sup>1</sup>H NMR chemical shifts of **1** indicated its nonaromatic conjugation character, including the peaks of  $\beta$  protons at 6.41, 6.51, 6.75, and 6.80 ppm. In contrast, peaks for pyridyl protons were observed at downfield-shifted range (7.75 and 8.31 ppm), reflecting its electron-deficient aromatic 6 $\pi$  conjugation circuit of the pyridine ring. Inner NH protons were observed at 5.06 ppm, which seems to be derived from fast tautomeric exchange with protons of water in CDCl<sub>3</sub>.<sup>13</sup>

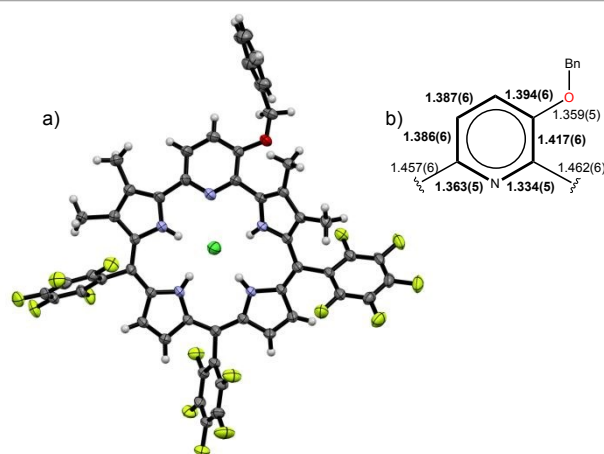
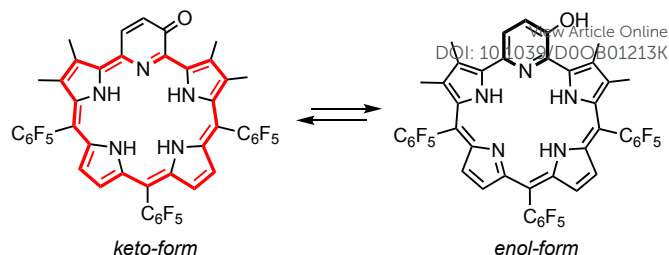


Fig. 2. X-ray crystal structure of 3-benzyl-oxypyripyentaphyrin **1**•HCl. a) Top view and b) selected bond lengths of the pyridine unit shown in Å. Solvent molecules and *meso*-aryl groups in side view were omitted. The thermal ellipsoids are shown at the 50% probability level.

The structure of **1** was unambiguously determined by X-ray crystallographic analysis.<sup>14</sup> The X-ray crystal structure was obtained in the protonated form with the counter chloride anion, as generated by 1,2-dichloroethane employed as the crystallisation solvent. In the X-ray crystal structure of pyridine ring of **1**, the pyridine ring showed C–C bond lengths in the range of 1.386(6)–1.417(6) Å, which were typical of aromatic C–C bonds. The C–N bond lengths of the pyridine ring were 1.334(5) and 1.345(7) Å, indicating its aromatic character. (Fig. 2b).

We conducted deprotection of benzyl group of **1** using hydrogenation under Pd/C catalysis, which proceeded almost quantitatively (Scheme 2). Simple chromatographic separation followed by recrystallisation furnished **2** in 78% yield. HR-ESI-TOF-MS analysis of **2** showed a peak at  $m/z$  = 946.1691 (calcd for  $C_{46}H_{22}N_5F_{15}O_1$ : 946.1663), which indicated the expected benzyl group removal. The NMR spectrum of **2** in  $CDCl_3$  clearly showed downfield-shifted  $\beta$ -protons in the range of 7.8–8.2 ppm, although complete characterisation of them was not easy because of its broadened peaks (Fig. S13). This broad NMR spectrum might be attributed to fast equilibrium of keto and enol forms of **2** (Scheme 3).<sup>8d</sup> The NMR peaks did not sharpen even at lower or higher temperature. However, in  $CD_3OD$ , highly downfield-shifted peaks belonging to pyrrole- $\beta$  protons were clearly observed at 7.87–8.23 ppm, indicating the aromatic character. The peak for the  $\beta$ -proton of 3-pyridone unit was highly downfield-shifted to 9.67 ppm owing to the diatropic ring current of the  $22\pi$  conjugation circuit and electron-withdrawing effect of the conjugated carbonyl group (Fig. S14). These data support the increased contribution of keto-form in protic solvents, as known in the tautomerism between the 4- and 2- pyridone derivatives.<sup>15</sup> In X-ray crystal structure of **2**<sup>16</sup> grown from the slow diffusion of hexane into chloroform solution was determined to be keto-form with four amine-type pyrrolic nitrogen atoms (Fig. 3). All pyrrole and pyridone units were inward-pointing. The detailed X-ray crystallographic structure showed a 1.278(6) Å of C–O bond, indicating strong double-bond character of **2**. In the 3-oxypyridine ring, C–N bond lengths were 1.345(6) and 1.352(6) Å, indicating retained aromatic bond character, while the bond-length alternation of C–C bonds was larger than those of **1**, at three 1.448(7), 1.439(8), 1.428(7) Å of single C–C bonds and 1.360(7) Å for one double C–C bond, suggesting the keto-form of **2** in the solid state. Furthermore, the pyridine–pyrrole C–C bond lengths were 1.434(7) and 1.433(7) Å, which is shortened to the aromatic bond length region compared with those in **1** (1.462(6) and 1.457(6) Å). The harmonic oscillator model of aromaticity (HOMA)<sup>17</sup> value for the overall  $22\pi$  macrocyclic structure of **2** was 0.71, which was larger than that of the cross-conjugated macrocyclic pathway of **1** calculated as 0.56 (Fig. S16). The mean plane deviation (MPD) of the pentaphyrin skeleton of **2** was calculated as 0.33 Å suggesting relatively planar structure of **2** than that of **1** with 0.46 Å of MPD. (Fig. 4).



Scheme 3. Keto-enol tautomerisation of **2**.

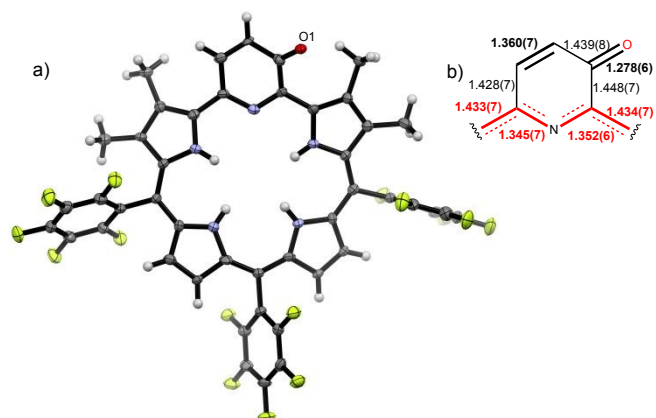


Fig. 3. X-ray crystal structure of 3-oxypyridine **2**. a) Top view b) selected bond lengths shown in Å. The solvent molecules and *meso*-aryl groups in side view were omitted. The thermal ellipsoids are shown at the 50% probability level.

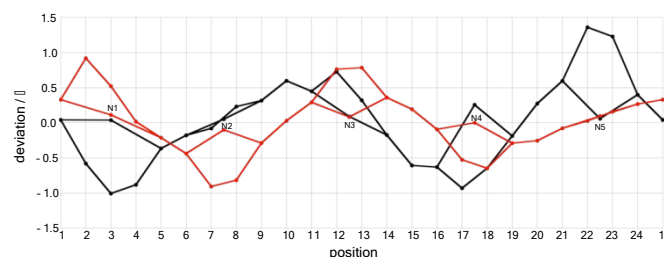


Fig. 4. Mean-plane deviation diagram calculated from the 29 core atoms for X-ray crystal structures of **1**(black) and **2**(red).

The aromaticity and strong NIR absorption of **2** was confirmed by its UV/Vis absorption spectra (Fig. 5). The absorption spectrum of **1** showed a relatively broad Soret-like band at 435 nm and almost no Q-like bands, suggesting its nonaromatic characteristics. However, **2** in dichloromethane, showed a similar the overall absorption spectrum shape, except for weak absorption bands at 437, 497, 519, 716 and 842 nm, which can be assigned as  $22\pi$  conjugation circuit. Furthermore, in methanol, all these peaks showed increased intensity, with a high molar coefficient observed. In particular, the strong Q-like absorption band at 852 nm with absorption coefficient of  $4.2 \times 10^4 \text{ M}^{-1}\text{cm}^{-1}$  suggested the suitability of this compound as an NIR photosensitiser.



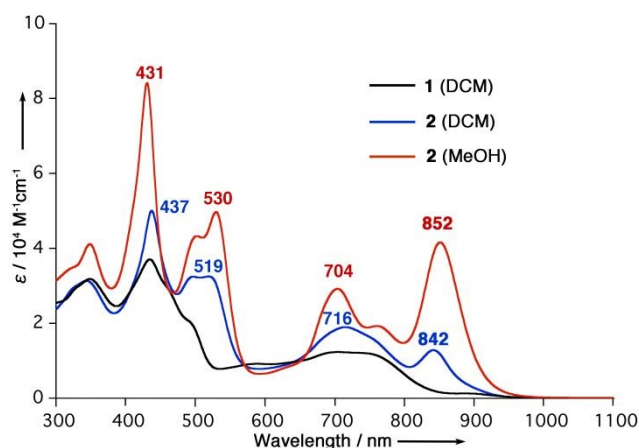


Fig. 5. UV/Vis absorption spectra of **1** in dichloromethane (black) and **2** in dichloromethane (blue) and **2** in methanol (red).

To investigate the aromaticity of **2**, we conducted DFT calculation<sup>18</sup> (B3LYP/6-31G level) on the keto- and enol forms of **2**. The aromaticity of the keto-form of **2** was supported by the calculated nucleus-independent chemical shifts (NICS(0)) value<sup>19</sup> of  $-10.91$  ppm at the gravity point of the macrocycle. In contrast, those of **1** and the enol-form of **2** were calculated to be  $-0.66$  and  $-0.73$  ppm, respectively, indicating nonaromatic characters. Meanwhile, the NICS(0) values of the six-membered ring in **1** and the enol-form of **2** were  $-9.73$  and  $-9.98$  ppm, respectively, owing to their  $6\pi$ -electron aromaticity, while that of the keto-form of **2** was  $+4.08$  ppm because the point was not the centre of a  $6\pi$  ring but the outside periphery of a  $22\pi$  macrocycle. The keto-form of **2** was slightly ( $16.7$  kJ/mol) more stable than that of enol-form though the HOMO-LUMO gaps of **1** and keto- and enol forms of **2** were very similar ( $1.97$ – $2.00$  eV). As observed in cyclic voltammograms with similar HOMO-LUMO gaps of **1** and **2** ( $1.45$ – $1.40$  eV, see ESI).

In conclusion, we have synthesised benzyl-group-protected pyripentaphyrin **1** and demonstrated its deprotection using hydrogenation to produce 3-oxypyripentaphyrin **2**. The transformation from nonaromatic **1** to aromatic **2** drastically induced aromaticity in the  $22\pi$  conjugation system, preserving its stability. The aromaticity of **2** was enhanced in methanol, with strong NIR absorption observed. Therefore, we have demonstrated the potential of expanded pyriporphyrins as theoretically promising candidates for photosensitizers.

## Conflicts of interest

There are no conflicts to declare.

## Acknowledgements

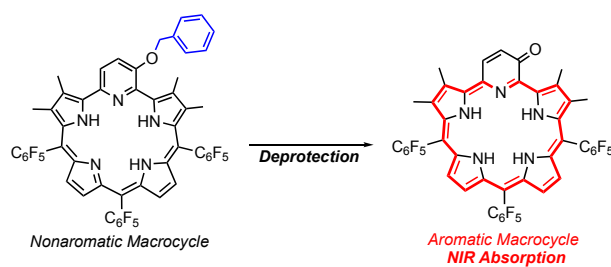
The work at Chiba was supported by JSPS KAKENHI. This work was supported by a JSPS KAKENHI grant for young scientists No. 17K14445(B) from MEXT of Japan and The Inohana Foundation.

## Notes and references

- (a) D. Dolmans, D. Fukumura, R. K. Jain, *Nat. Rev. Cancer*, 2003, **3**, 380–387; (b) J. Zhang, C. Jiang, J. P. F. Longo, R. B. Azevedo, H. Zhang, L. A. Muehlmann, A. *Pharm. Sin. B*, 2018, **8**, 137–146; (c) J. Kou, D. Dou, L. Yang, *Oncotarget*, 2017, **8**, 81591–81603.
- (a) N. M. Idris, M. K. Gnanasammandhan, J. Zhang, P. C. Ho, R. Mahendran, Y. Zhang, *Nat. Med.* 2012, **18**, 1580–1585; (b) J. M. Frangioni, *Curr. Opin. Chem. Biol.* 2003, **7**, 626–634.
- (a) J. L. Sessler, D. Seidel, *Angew. Chem. Int. Ed.* 2003, **42**, 5134–5175; (b) T. K. Chandrashekar, S. Venkatraman, *Acc. Chem. Res.* 2003, **36**, 676–691; (c) M. Stepien, N. Sprutta, L. Latos-Grażyński, *Angew. Chem. Int. Ed.* 2011, **50**, 4288–4340; (d) S. Saito, A. Osuka, *Angew. Chem. Int. Ed.* 2011, **50**, 4342–4373; (e) T. Tanaka, A. Osuka, *Chem. Rev.* 2017, **117**, 2584–2640; (f) B. Szyszko, M. J. Bialek, E. Pacholska-Dudziak, L. Latos-Grażyński, *Chem. Rev.* 2017, **117**, 2839–2909; (g) T. Chatterjee, A. Srinivasan, M. Ravikanth, T. K. Chandrashekar, *Chem. Rev.* 2017, **117**, 3329–3376.
- (a) J. L. Sessler, N. A. Tvermoes, J. Davis, P. Anzenbacher Jr, K. Jursicová, W. Sato, D. Seidel, V. Lynch, C. B. Black, A. Try, B. Andrioletti, G. Hemmi, T. D. Mody, D. J. Magda, V. Král, *Pure. Appl. Chem.* 1999, 2009–2018; (b) C. Comuzzi, S. Cogoi, M. Overhand, G. A. V. Marel, H. S. Overleef, L. E. Xodo, *J. Med. Chem.* 2006, **49**, 196–204; (c) C. S. Gutsche, M. Ortwerth, S. Gräfe, K. J. Flanagan, M. O. Senge, H.-U. Reissig, N. Kulak, A. Wiehe, *Chem. Eur. J.* 2016, **22**, 13953–13964.
- (a) J. L. Sessler, J. M. Davis, V. Lynch, *J. Org. Chem.* 1998, **63**, 7062–7065; (b) J. L. Sessler, D. Seidel, C. Bucher, V. Lynch, *Tetrahedron*, 2001, **57**, 3743–3752; (c) Z. S. Yoon, D.-G. Cho, K. S. Kim, J. L. Sessler, D. Kim, *J. Am. Chem. Soc.* 2008, **130**, 6930–6931.
- (a) K. Berlin, E. Breitmaier, *Angew. Chem. Int. Ed. Engl.* 1994, **33**, 219–220; (b) R. Myśliborski, L. Latos-Grażyński, L. Sztrenberg, *Eur. J. Org. Chem.* 2006, 3064–3068.
- (a) T. D. Lash, S. T. Chaney, *Chem. Eur. J.* 1996, **2**, 944–948; (b) T. Shronemeier, E. Breitmaier, *Synthesis*, 1997, 273; (c) T. D. Lash, S. T. Chaney, D. T. Richter, *J. Org. Chem.* 1998, **63**, 9076–9088; (d) D. Liu, G. M. Ferrence, T. D. Lash, *J. Org. Chem.* 2004, **69**, 6079–6093; (e) T. D. Lash, K. P. Pokharel, J. M. Serling, V. R. Yant, G. M. Ferrence, *Org. Lett.* 2007, **9**, 2863–2866; (f) S. Neya, M. Suzuki, H. Ode, T. Hoshino, Y. Furutani, H. Kandori, H. Hori, K. Imai, T. Komatsu, *Inorg. Chem.* 2008, **47**, 10771–10778; (g) S. Neya, M. Suzuki, T. Mochizuki, T. Hoshino, A. T. Kawaguchi, *Eur. J. Org. Chem.* 2015, 3824–3829.
- (a) J.-i. Setsune, K. Watanabe, *J. Am. Chem. Soc.* 2008, **130**, 2404–2405; (b) J.-i. Setsune, K. Yamato, *Chem. Commun.* 2012, **48**, 4447–4449.
- D. T. Richter, T. D. Lash, *Tetrahedron*, 2001, **57**, 3657–3671.
- (a) Z. Zhang, J. M. Lim, M. Ishida, V. V. Roznyatovsky, V. M. Lynch, H.-Y. Gong, X. Yang, D. Kim, J. L. Sessler, *J. Am. Chem. Soc.* 2012, **134**, 4076–4079; (b) Z. Chang, W.-Y. Cha, N. J. Williams, E. L. Rush, M. Ishida, V. M. Lynch, D. Kim, J. L. Sessler, *J. Am. Chem. Soc.* 2014, **136**, 7591–7594.
- D. Mori, T. Yoneda, M. Suzuki, T. Hoshino, S. Neya, *Chem. Asian. J.* 2019, **14**, 4169–4173.
- J.-i. Setsune, M. Toda, K. Watanabe, P. K. Panda, T. Yoshida, *Tetrahedron Lett.* 2006, **47**, 7541–7544.
- K. Rachlewicz, L. Latos-Grażyński, A. Hebauer, A. Vivian, J. L. Sessler, *J. Chem. Soc. Parkin Trans 2*, 1999, 2189–2195.
- X-ray data for **1**•HCl: ( $C_{53}H_{29}F_{15}N_5O_1$ )•HCl•2(1,2-dichloroethane) ( $M_r = 1171.22$ ), triclinic, space group  $P_1$  (No. 2),  $a = 13.2433(3)$ ,  $b = 13.7134(3)$ ,  $c = 15.7312(4)$  Å,  $\alpha = 70.848(1)^\circ$ ,  $\beta = 80.596(1)^\circ$ ,  $\gamma = 66.090(1)^\circ$ ,  $V = 2465.69(10)$  Å<sup>3</sup>,  $Z = 2$ ,  $\rho_{\text{calcd}} = 1.577$  g cm<sup>-3</sup>,  $T = 93(2)$  K,  $R_1 = 0.0841$  ( $I > 2\sigma(I)$ ),  $wR_2 = 0.2495$  (all data), GOF = 1.120. CCDC 1996098 contains the supplementary crystallographic data for this paper. These data are provided free of charge by the Cambridge Crystallographic Data Centre.

- 15 A. Gordon, A. R. Katritzky, *Tetrahedron Lett*, 1968, **23**, 2767–2770.
- 16 X-ray data for **2**: (C<sub>46</sub>H<sub>22</sub>F<sub>15</sub>N<sub>5</sub>O<sub>1</sub>)•2(chloroform) (Mr = 1184.42), monoclinic, space group *P*-1 (No. 2), *a* = 12.2776(3), *b* = 13.0559(3), *c* = 16.5083(4) Å,  $\alpha$  = 105.241(1)°,  $\beta$  = 110.613(1)°,  $\gamma$  = 98.939(2)°, *V* = 2297.85(10) Å<sup>3</sup>, *Z* = 2,  $\rho_{\text{calcd}}$  = 1.712 gcm<sup>-3</sup>, *T* = 93(2) K, *R*<sub>1</sub> = 0.0965 (*I* > 2σ(*I*)), *wR*<sub>2</sub> = 0.2705 (all data), GOF = 0.1049. CCDC 1996099 contains the supplementary crystallographic data for this paper. These data are provided free of charge by the Cambridge Crystallographic Data Centre.
- 17 (a) T. M. Krygowski, T. M. Cryański, *Tetrahedron* 1996, **52**, 1713–1722; (b) T. M. Krygowski, T. M. Cryański, *Tetrahedron* 1996, **52**, 10255–10264.
- 18 Gaussian 09, Revision A.02, M. J. Frisch. et al., Gaussian, Inc., Wallingford, CT, 2009 (Full citation in SI).
- 19 (a) P. v. R. Schleyer, C. Maerker, A. Dransfeld, H. Jiao, N. J. R. v. E. Hommes, *J. Am. Chem. Soc.* 1996, **118**, 6317–6318; (b) Z. Chen, C. S. Wannere, C. Corminboeuf, R. T. Puchta, P. v. R. Schleyer, *Chem. Rev.* 2005, **105**, 3842–3888.

View Article Online  
DOI: 10.1039/D0OB01213K



We report a deprotection-induced aromaticity switching from nonaromatic to 22n aromatic macrocycle of 3-oxopyrripentaphyrin(0.1.1.1.0) with strong NIR absorption.